Turk Neurosurg 36(4):608-614, 2026
DOI: 10.5137/1019-5149.JTN.49391-25.2

Case Report

Received: 04.07.2025
Accepted: 09.08.2025

Published Online: 24.07.2026

Recurrent and De Novo Internal Carotid Artery Aneurysms with Severe Stenosis Following Radiation Therapy for Nasopharyngeal Carcinoma: A Rare Case Report

Xiaohui XU, Yongjun TAO, Lingling QIU

Taizhou Municipal Hospital (Taizhou University Affiliated Municipal Hospital), School of Medicine, Taizhou University, Department of Neurology, Taizhou, China

Corresponding author: Lingling QIU ✉ qiulingling0110@126.com

ABSTRACT

Rapid formation and recurrence of aneurysms accompanied by severe arterial stenosis following radiation therapy (RT) for nasopharyngeal carcinoma (NPC) is an uncommon clinical phenomenon. We present the case of a 51-year-old man who developed subarachnoid hemorrhage years after undergoing RT for NPC. Digital subtraction angiography revealed a ruptured, irregular, wide-neck aneurysm at the posterior communicating segment of the right internal carotid artery (ICA), along with significant stenosis (approximately 80%) at the cervical segment of the same artery. The cervical ICA stenosis was initially treated with stenting, followed by LVIS stent-assisted coil embolization of the aneurysm. Over the next four years, the patient developed three entirely new ICA aneurysms—one of which arose from within the middle portion of the previously placed LVIS stent (a finding not previously reported)—as well as one recurrent aneurysm. This rare case highlights the dynamic nature of RT-induced ICA aneurysm formation and recurrence. Lifelong monitoring and individualized endovascular management are crucial. Considering the fragility of irradiated tissues, extensive arterial involvement, and increased surgical risk from repeat procedures, endovascular treatment was favored over open surgery.

KEYWORDS: Radiation therapy, Endovascular treatment (EVT), Nasopharyngeal carcinoma (NPC), Intracranial aneurysm, Recurrence

ABBREVIATIONS: RT: Radiation therapy, **NPC:** Nasopharyngeal carcinoma, **ICA:** Internal carotid artery, **CT:** Computed tomography, **SAH:** Subarachnoid hemorrhage, **DSA:** Digital subtraction angiography, **aSAH:** Aneurysmal subarachnoid hemorrhage, **CTA:** Computed tomography angiography, **EVT:** Endovascular treatment, **GCS:** Glasgow Coma Scale

INTRODUCTION

Nasopharyngeal carcinoma (NPC) is predominantly a squamous cell carcinoma arising from the columnar epithelium of the nasopharynx, with a marked geographic prevalence in Southeast and East Asia (4). Radiation therapy (RT) remains the cornerstone of NPC treatment and has significantly improved patient survival (7). However, its potential adverse effects on cerebral vasculature are increasingly recognized. Although RT-induced aneurysms are rare, they can lead to aneurysmal subarachnoid hemorrhage (aSAH)—a severe and often fatal complication associated with high morbidity and mortality rates (3). Considering these risks, greater clinical attention should be directed toward the detection and management of RT-related aneurysms.

Intracranial aneurysms following RT for NPC occur at an estimated incidence of 47.8 per 100,000 person-years (15). However, the sequential development and rupture of multiple new and recurrent internal carotid artery (ICA) aneurysms

Xiaohui XU : 0009-0003-0289-2006 Yongjun TAO : 0000-0002-4666-6743 Lingling QIU : 0000-0002-3215-2338

within a relatively short time frame—particularly in the setting of severe post-RT ICA stenosis—remains exceedingly rare in clinical reports. We present the case of a 51-year-old man with a history of RT for NPC who developed three entirely new ICA aneurysms and one recurrent aneurysm over a 4-year period. Notably, this case represents the first reported instance of an aneurysm arising from the mid-segment of an LVIS stent coverage zone—a previously undocumented phenomenon with important implications for endovascular treatment in irradiated vessels. Through detailed angiographic follow-up and hemodynamic analysis, this case offers rare insights into the progressive nature of radiation-induced vasculopathy. Our findings highlight the urgent need for evidence-based surveillance strategies and tailored therapeutic approaches for managing these complex and evolving vascular complications.

CASE REPORT

A 51-year-old man was diagnosed with NPC in 2008, confirmed pathologically as undifferentiated carcinoma (Figure 1). He underwent chemotherapy and RT, receiving 2 Gy per session over 30 sessions, for a total dose of 60 Gy. Following several years of radiological, clinical, and oncological surveillance, he achieved complete remission. His medical history included hypertension, intermittent headaches, and a 10-year history of smoking.

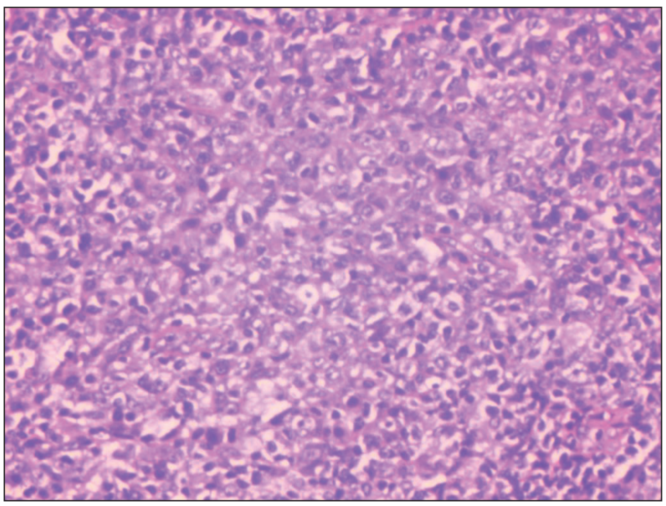

Figure 1: Histopathological examination confirmed undifferentiated nasopharyngeal carcinoma, visualized using Hematoxylin and Eosin stain, ×40 magnification.

First Admission (August 2017): The patient was admitted to our hospital with a 3-day history of headache. Neurological examination showed nuchal rigidity, with no other abnormal findings. Emergency computed tomography (CT) at admission revealed SAH (Figure 2A), and CT angiography (CTA) revealed approximately 80% eccentric stenosis accompanied by a dissecting aneurysm at the cervical segment of the right ICA (Figure 2B). Digital subtraction angiography (DSA) further identified a ruptured, wide-neck, irregular aneurysm at the posterior communicating segment of the right ICA (Figure 2C), with no abnormalities in other cerebral vessels. Given the significant cervical ICA stenosis that could hinder endovascular treatment (EVT), a self-expanding Xact stent (Abbott Vascular, Abbott Park, IL, USA) was first deployed in the affected segment. Subsequently, the ruptured aneurysm was successfully embolized using coils with assistance from an LVIS stent (MicroVention, Tustin, CA, USA). Post-procedural angiography confirmed complete occlusion of the aneurysm with no residual neck (Figure 2D, E). The patient recovered well and was discharged without any neurological deficits.

Second Admission (February 2019): Eighteen months later, the patient was readmitted to our hospital due to impaired consciousness. Immediate brain CT revealed SAH (Figure 3A). DSA detected a newly formed, wide-neck, irregular ruptured aneurysm located at the choroidal segment of the left ICA (Figure 3B, C). This aneurysm had not been present on the initial DSA, and the previously treated aneurysm remained stable, with no signs of recurrence or neck remnant. No additional aneurysms were identified. Considering the successful outcome of the prior EVT, the patient's family opted for the same therapeutic approach. Under general anesthesia, the newly ruptured aneurysm was embolized using coils with the assistance of an LVIS stent. Post-procedure DSA showed a small residual neck (Figure 3D, E). The patient made a full recovery and was discharged without neurological deficits or complications.

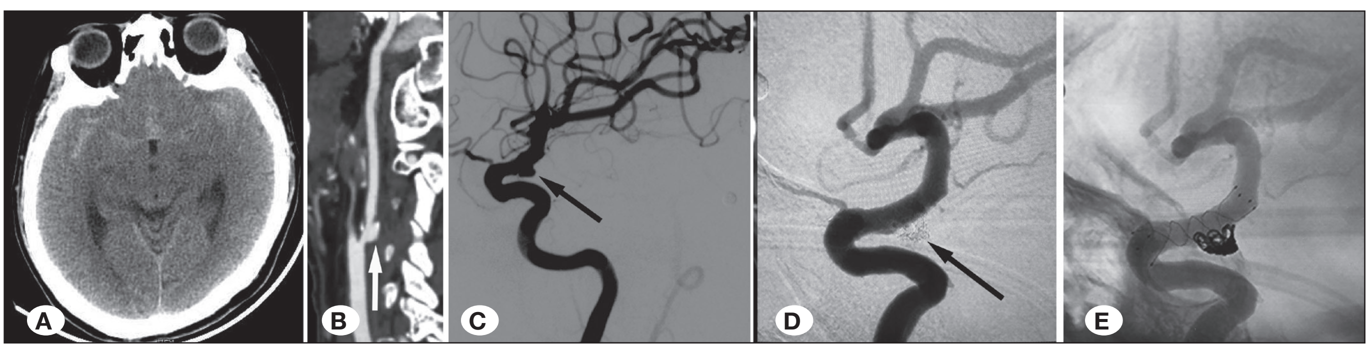

Figure 2: Images of the first procedure (August 2017). **A)** Brain CT revealed subarachnoid hemorrhage. **B)** CTA revealed approximately 80% eccentric stenosis with a dissecting aneurysm at the cervical segment of the right internal carotid artery. **C)** DSA revealed a ruptured, wide-neck, irregular aneurysm at the posterior communicating segment of the right ICA. **D, E)** Immediate post-procedural angiography confirmed complete occlusion with no residual neck.

Third Admission (March 2019): Only 1 month after the second procedure, the patient experienced a third episode of aSAH, presenting with a Hunt–Hess grade of 3 and a Glasgow Coma Scale score of 9 upon admission. Emergency brain CT revealed SAH accompanied by hydrocephalus (Figure 4A). Subsequent DSA showed that the previously treated aneurysm at the choroidal segment of the left ICA remained stable, with no signs of recurrence (Figure 4B). However, a newly developed pseudoaneurysm was identified at the choroidal segment of the right ICA, which had not been present in prior imaging (Figure 4C). No additional aneurysms were detected. Following multidisciplinary consultation and consensus on treatment strategy, the new aneurysm was embolized using LVIS stent-assisted coils, and external ventricular drainage of the right lateral ventricle was performed. Immediate and 20-day follow-up DSA confirmed complete occlusion of the aneurysm with no residual neck (Figure 4D, E). Although recovery was slow, the patient was eventually discharged with limited functional independence but able to manage basic self-care.

Fourth Admission (January 2021): Over time, the patient's neurological deficits related to hydrocephalus gradually improved. However, he was readmitted to our institution with complaints of intermittent headaches lasting 4 days. Emergency brain CT showed no evidence of SAH but revealed mild hydrocephalus (Figure 5A). Considering his complex medical history, a routine DSA was performed. The angiography confirmed no recurrence of the previously treated aneurysms at the posterior communicating and choroidal segments of the right ICA (Figure 5B). Remarkably, however, the coils from the second treated aneurysm had shifted from their original position at the choroidal segment of the left ICA (Figure 5C). Furthermore, a third new aneurysm had developed at the posterior communicating segment of the left ICA (Figure 5D, E). Due to the wide-necked and irregular morphology of the new aneurysm, along with fragility of the parent vessel, the patient was pretreated with daily aspirin (100 mg) and clopidogrel (75 mg) for approximately 1 week before the procedure. Subsequently, both aneurysms were successfully treated with LVIS stent-assisted coil embolization (Figure 5F, G). No new neurological deficits were observed during the perioperative period, and the patient was discharged uneventfully. Ongoing neuroimaging and clinical monitoring have been maintained diligently.

Fifth Admission (November 2021): During the most recent follow-up in November 2021, DSA revealed a recurrence of the aneurysm at the choroidal segment of the left ICA (Figure 6A), likely associated with a small neck remnant from the previously treated lesion. To address this, an additional LVIS stent was deployed within the existing stent to reinforce coverage of the aneurysm neck, without performing coil embolization (Figure 6B). Immediate post-procedural DSA demonstrated intra-aneurysmal contrast stagnation (Figure 6C). The patient was discharged without any new neurological deficits. A summary of the patient's clinical course is provided in Table I.

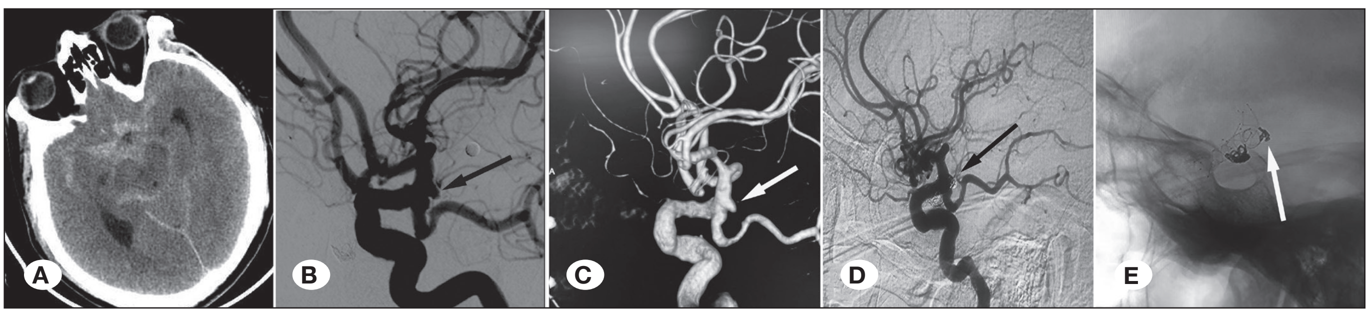

Figure 3: Images of the second procedure (February 2019). **A)** Brain CT revealed subarachnoid hemorrhage. **B, C)** DSA and three-dimensional DSA identified a wide-neck, ruptured, irregular aneurysm at the choroidal segment of the left ICA. **D, E)** Post-procedure angiography performed immediately revealed a small neck remnant.

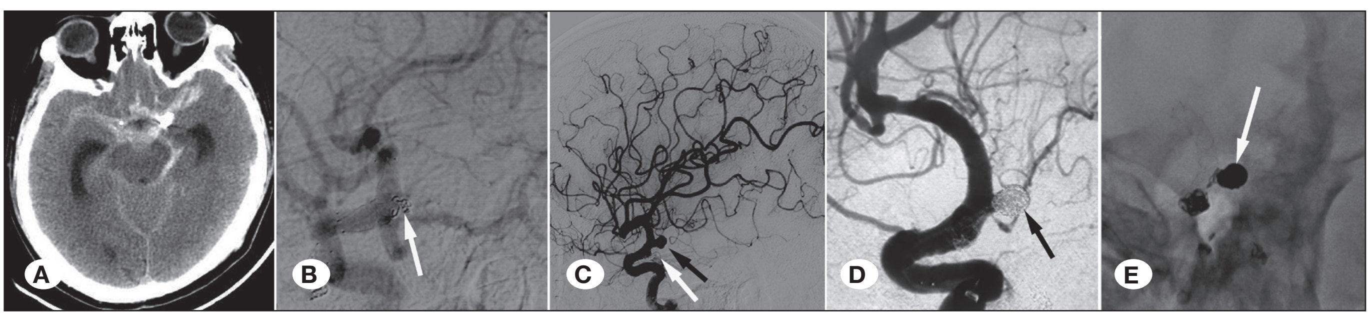

Figure 4: Images of the third procedure (March 2019). **A)** Brain CT indicated subarachnoid hemorrhage coupled with hydrocephalus. **B)** DSA revealed that the coils of the second treated aneurysm at the choroidal segment of the left ICA were in position. **C)** DSA revealed that the first treated aneurysm at the posterior communicating segment of the right ICA was stable(white arrow) and identified a newly developed pseudoaneurysm at the choroidal segment of the right ICA(black arrow). **D, E)** The postoperative DSA revealed complete occlusion of the aneurysm at the choroidal segment of the right ICA.

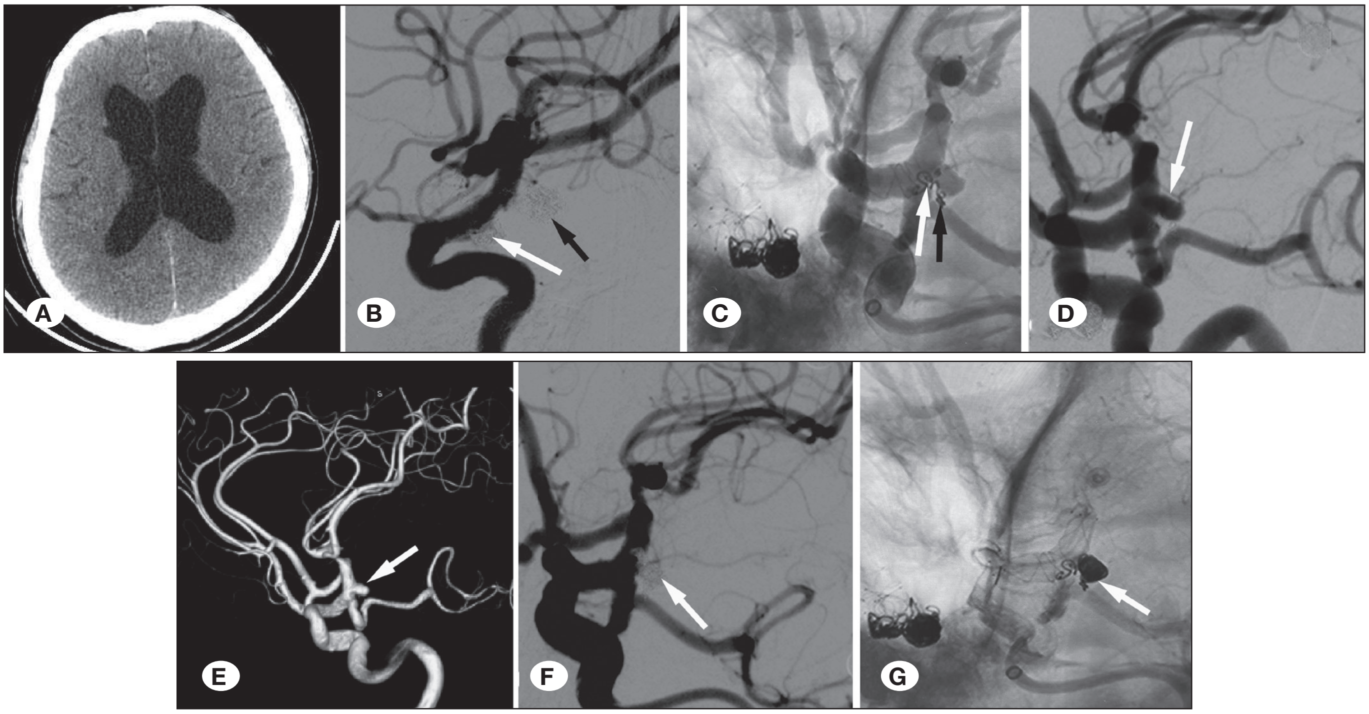

Figure 5: Images of the fourth procedure (January 2021). **A)** Brain CT revealed no sign of subarachnoid hemorrhage, but mild hydrocephalus. **B)** DSA revealed that the first (white arrow) and third (black arrow) treated aneurysms, respectively, at the posterior communicating and choroidal segments of the right ICA, were stable. **C)** DSA demonstrated that the coils of the second treated aneurysm at the choroidal segment of the left ICA were shifted from the previous position (shifting from the black arrow to the white arrow). **D, E)** DSA and 3D-DSA revealed a newly developed aneurysm at the posterior communicating segment of the left ICA. **F, G)** Postoperative DSA revealed complete occlusion of the aneurysms at the posterior communicating and choroidal segments of the left ICA.

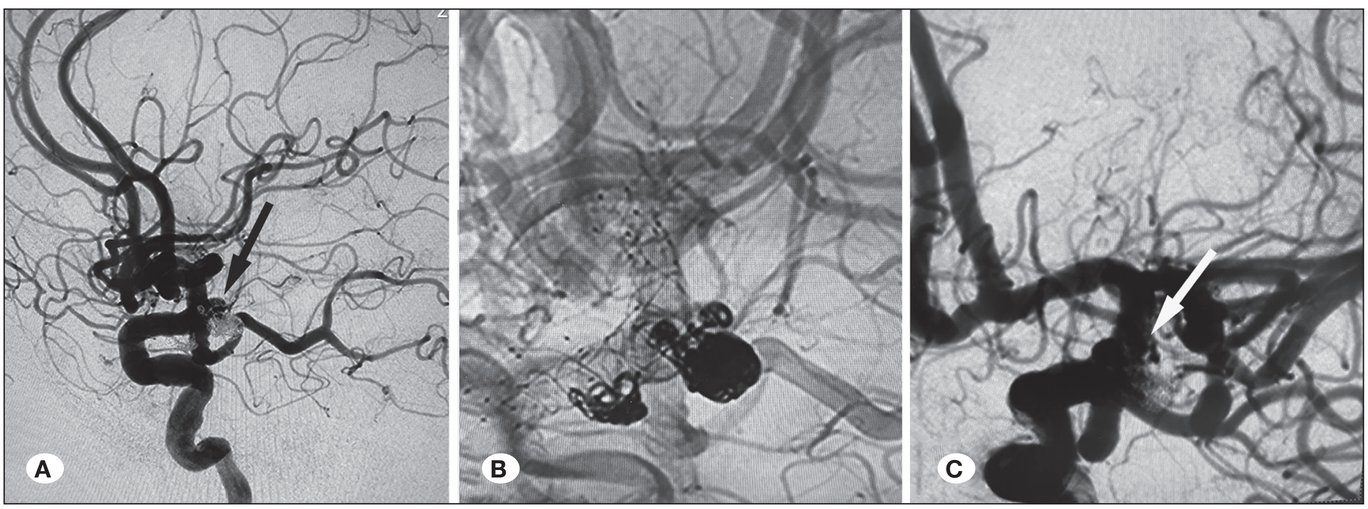

Figure 6: Images of the fifth procedure (November 2021). **A)** DSA indicated the recurrence of the aneurysm (black arrow) at the choroidal segment of the left ICA (the second treated aneurysm). **B)** DSA revealed that the LVIS stent was deployed to cover the aneurysm neck without coil embolization. **C)** The immediate postoperative DSA showed intra-aneurysmal contrast stasis (white arrow).

DISCUSSION

RT induces complex vascular injury through multiple interrelated mechanisms. These include endothelial dysfunction and chronic inflammation, which promote atherosclerosis and compromise vessel wall integrity (14); activation of molecular pathways, where ionizing radiation stimulates NF-κB and matrix metalloproteinases (MMPs), facilitating aneurysm development and rupture (6,8,10,13); impaired adventitial repair due to RT-induced fibroblast dysfunction (11); and hemodynamic stress, wherein altered shear forces exacerbate structural vessel fragility (9). The average latency between cancer

Table I: Timeline of Disease Progression of after Patient

Admission time	Symptom	Physical Examination	Hunt and Hess Scale (Grade)	GCS	CT scan	Lesion location	Procedure	Follow up time/ results	Measures
August 2017	Headache	Nuchal rigidity	1	15	SAH	Posterior communicating segment of the right ICA; 80% eccentric stenosis with dissecting aneurysm at the cervical segment of the right ICA	LVIS stent with coils, Xact stent	February 2019 (no recurrence) March 2019 (no recurrence) January 2021 (no recurrence) November 2021 (no recurrence)	DSA surveillance
February 2019	Impaired consciousness	Noncooperation	3	10	SAH	Choroidal segment of the left ICA (the first newly developed aneurysm)	LVIS stent with coils (a small neck remnant)	March 2019 (a small neck remnant, no recurrence) January 2021 (coils shifting) November 2021 (recurrence)	Surveillance LVIS stent with coils LVIS stent alone
March 2019	Headache	Nuchal rigidity	3	9	SAH with hydrocephalus	Pseudoaneurysm choroidal segment of the right ICA (the second newly developed aneurysm)	LVIS stent-assisted coils	January 2021 (no recurrence) November 2021 (no recurrence)	Surveillance Surveillance
January 2021	Intermittent headache	Slow response	0	15	No SAH but mild hydrocephalus	Posterior communicating segment of the left ICA (the third newly developed aneurysm)	LVIS stent with coils	November 2021 (no recurrence)	Surveillance

***GCS:** Glasgow coma scale, **CT:** computed tomography, **SAH:** subarachnoid hemorrhage, **LVIS:** low-profile visualized intraluminal support, **ICA:** internal carotid artery* diagnosis and intracranial aneurysm formation has been reported as 4.3 ± 3.1 years (15). However, this case is exceptionally rare—demonstrating the sequential formation of three entirely new aneurysms and one recurrence within just 4 years. In this patient, the compounding effects of hypertension and smoking-related atherosclerosis likely intensified RT-induced vascular damage. Although the primary NPC was localized in the nasopharynx, standard radiation fields often encompass the skull base and proximal intracranial arteries due to potential tumor spread along neural pathways. The dose-dependent relationship between RT and intracranial aneurysms is well documented: 1) the carotid siphon receives substantial scatter radiation during NPC treatment (typically 60–70 Gy to the primary tumor site) (15); 2) histological analyses have revealed similar features of radiation vasculopathy—such as vasa vasorum obliteration and medial necrosis—in both cervical and intracranial carotid segments (2); and 3) hemodynamic compensation for proximal stenosis, as seen in this patient's 80% cervical ICA narrowing, increases stress on distal arterial walls, thereby accelerating aneurysm formation in irradiated but non-stenotic intracranial regions (5).

Typically, LVIS stent-assisted coil embolization for small aneurysms carries a low recurrence rate, reported at 7.4% (12), and there have been no prior reports of new aneurysm formation within the stent-covered segments. Remarkably, this case represents the first documented instance of a de novo aneurysm arising from the mid-portion of an LVIS stent's coverage area (Figure 5D, E)—a novel and clinically significant event with important implications for endovascular device selection in radiation-compromised vasculature. In the context of post-RT vasculopathy, even unruptured aneurysms may warrant a lower threshold for intervention, though the choice between EVT and surgery must be individualized. Moreover, DSA revealed coil displacement in the previously treated aneurysm, likely due to inflammation-induced endothelial instability. Taking into account the patient's medical history, family preferences, and financial considerations, LVIS stent-assisted coil embolization was successfully performed for both aneurysms. However, during the most recent procedure (November 2021), the recurrent aneurysm was treated with an LVIS stent alone—without coils—to cover the aneurysm neck (Figure 6B), considering the risks of coil migration and potential compromise of the choroidal artery. Postoperative DSA showed contrast stagnation within the aneurysm sac (Figure 6C), suggesting effective flow diversion. In such complex cases, flow diverters may also serve as a viable alternative.

In summary, while LVIS stent-assisted coiling provided immediate aneurysm occlusion in RT-induced cases, its long-term durability was limited (Figure 6A, Figure 3D-E, and Figure 5G), and coil migration was observed at irradiated sites, likely due to ongoing inflammation and vascular remodeling (Figure 5C). Therefore, an adaptive treatment strategy was employed: for the recurrent aneurysm (Figure 6A-C), standalone LVIS stent placement—without coiling—was used to prioritize parent vessel reconstruction over direct aneurysm filling, achieving effective contrast stasis through flow diversion. This case yields several clinical insights: patients with NPC who have a history of smoking, hypertension, and received radiation doses exceeding 60 Gy should undergo lifelong vascular surveillance. We recommend follow-up DSA at 6, 12, and 24 months post-EVT. Regarding treatment approach, stent-assisted coiling remains a valid first-line option for primary aneurysms, whereas flow diverters may offer a superior alternative for recurrent lesions, particularly to prevent coil migration.

The consistent use of endovascular treatment in this case was guided by three primary factors: First, irradiated tissues are prone to poor wound healing and carry an increased risk of surgical complications, such as carotid blowout (1,2). Second, the stepwise development of aneurysms across multiple segments of the ICA—from cervical to intracranial—would necessitate overly extensive and invasive surgical exposure. Third, repeated open surgeries would impose significant cumulative morbidity, especially given the patient's radiation-induced tissue fibrosis (2). These considerations support the current clinical consensus, which favors endovascular intervention over open surgery for radiation-induced vasculopathy when anatomically feasible.

CONCLUSION

This case underscores the dynamic and recurrent nature of RT-induced internal carotid artery aneurysms. Despite achieving "complete" initial treatment, rigorous and ongoing angiographic monitoring is essential for early detection of de novo or recurrent lesions. In irradiated vasculature, endovascular strategies should shift from solely focusing on aneurysm occlusion to prioritizing vessel preservation and long-term vascular integrity.

Declarations

Funding: This research did not receive any specific grant from funding agencies in the public, commercial, or not-for-profit sectors.

Availability of data and materials: The datasets generated and/or analyzed during the current study are available from the corresponding author by reasonable request.

Disclosure: The authors declare no competing interests.

Ethics approval and consent to participate: This study was approved by the Ethics Committee of Taizhou Municipal Hospital (NO. LW011). Written informed consent was obtained from the patient.

AUTHORSHIP CONTRIBUTION

Study conception and design: XX, YT, LQ

Data collection: LQ

Analysis and interpretation of results: XX, YT, LQ

Draft manuscript preparation: LQ

Critical revision of the article: XX, LQ

Other (study supervision, fundings, materials, etc...): XX, YT, LQ

All authors (XX, YT, LQ) reviewed the results and approved the final version of the manuscript.

REFERENCES

1. Anil G, Zhang J, Ong YK, Hui F: Flow-diverter in radiation-induced skull base carotid blowout syndrome: Do not write it off!. Neurosurg Rev 40:685-688, 2017. https://doi.org/10.1007/s10143-017-0875-3
2. Denham JW, Hauer-Jensen M: The radiotherapeutic injury-a complex 'wound'. Radiother Oncol 63:129-145, 2002. https://doi.org/10.1016/s0167-8140(02)00060-9
3. Dharia A, Lacci JV, Mascitelli J, Seifi A: Impact of ruptured aneurysm circulation on mortality: A nationwide inpatient sample analysis. J Stroke Cerebrovasc Dis 29:105124, 2020. https://doi.org/10.1016/j.jstrokecerebrovasdis.2020.105124
4. Guo R, Mao YP, Tang LL, Chen L, Sun Y, Ma J: The evolution of nasopharyngeal carcinoma staging. Br J Radiol 92: 20190244, 2019. https://doi.org/10.1259/bjr.20190244
5. Kono K, Fujimoto T, Terada T: Proximal stenosis may induce initiation of cerebral aneurysms by increasing wall shear stress and wall shear stress gradient. Int J Numer Method Biomed Eng 30:942-950, 2014. https://doi.org/10.1002/cnm.2637
6. Kumagai T, Rahman F, Smith AM: The microbiome and radiation induced-bowel injury: evidence for potential mechanistic role in disease pathogenesis. Nutrients 10: 1405, 2018. https://doi.org/10.3390/nu10101405
7. Liao W, Zheng Y, Bi S, Zhang B, Xiong Y, Li Y, Fang W, Xiao S, Yang L, Thea A, Liu J: Carotid stenosis prevalence after radiotherapy in nasopharyngeal carcinoma: A meta-analysis. Radiother Oncol 133:167-175, 2019. https://doi.org/10.1016/j.radonc.2018.11.013
8. Mussbacher M, Salzmann M, Brostjan C, Hoesel B, Schoergenhofer C, Datler H, Hohensinner P, Basilio J, Petzelbauer P, Assinger A, Schmid JA: Cell type-specific roles of NF-kappaB linking inflammation and thrombosis. Front Immunol 10:85, 2019. https://doi.org/10.3389/fimmu.2019.00085
9. Nanney AR, El TN, El AT, Daou MR, Bit IE, Marymont MH, Batjer HH, Bendok BR: Intracranial aneurysms in previously irradiated fields: Literature review and case report. World Neurosurg 81:511-519, 2014. https://doi.org/10.1016/j.wneu.2013.10.044
10. Rojas HA, Fernandes K, Ottone MR, Magalhaes K, Albuquerque L, Pereira J, Vieira-Junior G, Sousa-Filho JL, Costa BS, Sandrim VC, Dellaretti M, Simoes RT: Levels of MMP-9 in patients with intracranial aneurysm: Relation with risk factors, size and clinical presentation. Clin Biochem 55:63-68, 2018. https://doi.org/10.1016/j.clinbiochem.2018.03.005
11. Sciubba DM, Gallia GL, Recinos P, Garonzik IM, Clatterbuck RE: Intracranial aneurysm following radiation therapy during childhood for a brain tumor. Case report and review of the literature. J Neurosurg 105:134-139, 2006. https://doi.org/10.3171/ped.2006.105.2.134
12. Settipalli KP, Dunkerton S, Hilton J, Aw G, Lock G, Mitchell K, Coulthard A: The ELVIS study: Medium and long-term Efficacy of LVIS EVO stent-assisted coil embolisation for unruptured saccular intracranial aneurysms-A tertiary single-centre experience. J Med Imaging Radiat Oncol 69:212-220, 2025. https://doi.org/10.1111/1754-9485.13820
13. Weintraub NL, Jones WK, Manka D: Understanding radiation-induced vascular disease. J Am Coll Cardiol 55:1237-1239, 2010. https://doi.org/10.1016/j.jacc.2009.11.053
14. Venkatesulu BP, Sanders KL, Hsieh CE, Kim BK, Krishnan S: Biomarkers of radiation-induced vascular injury. Cancer Rep (Hoboken) 2:e1152, 2019. https://doi.org/10.1002/cnr2.1152
15. Yang WH, Yang YH, Chen PC, Wang TC, Chen KJ, Cheng CY, Lai CH: Intracranial aneurysms formation after radiotherapy for head and neck cancer: A 10-year nationwide follow-up study. Bmc Cancer 19:537, 2019. https://doi.org/10.1186/s12885-019-5766-2